Metal enhanced fluorescence on nanoporous gold leaf-based assay platform for virus detection

Metal enhanced fluorescence on nanoporous gold leaf-based assay platform for virus detection

Syed Rahin Ahmed[a, b], Md Ashraf Hossain[b], Jung Youn Park[c], Soo-Hyung Kim[b], Dongyun Lee[d], Tetsuro Suzuki[e], Jaebeom Lee[d*], and Enoch Y. Park[a, f*]

[a] *Graduate School of Science and Technology, Shizuoka University, 836 Ohya Suruga-ku, Shizuoka 422-8529, Japan*

[b] *Department of Nano Fusion Technology, Pusan National University, Miryang 627-706, Republic of Korea*

[c] *National Fisheries Research and Development Institute, Busan 619-705, Republic of Korea*

[d] *Department of Nano Fusion Engineering and Cogno-Mechatronics Engineering, Pusan National University, Busan, 609-735, Korea*

[e] *Department of Infectious Diseases, Hamamatsu University School of Medicine, 1-20-1 Higashi-ku, Handa-yama, Hamamatsu 431-3192, Japan*

[f] *Research Institute of Green Science and Technology, Shizuoka University, 836 Ohya Suruga- ku, Shizuoka, 422-8529, Japan*

rahin_sust@yahoo.com (SRA)

ashraf3521@gmail.com (MAH)

jypark@nfrdi.go.kr (JYP)

sookim@pusan.ac.kr (SHK)

dlee@pusan.ac.kr (DL)

tesuzuki@hama-med.ac.jp (TS)

jaebeom@pusan.ac.kr (JL)

acypark@ipc.shizuoka.ac.jp (EYP)

_____

[*] Correspondence to: Research Institute of Green Science and Technology, Shizuoka University, 836 Ohya Suruga- ku, Shizuoka, 422-8529, Japan. Tel. & fax: +81 54 238 4887. *E-mail address:* acypark@ipc.shizuoka.ac.jp (EYP); Department of Nano Fusion Engineering and Cogno-Mechatronics Engineering, Pusan National University, Busan, 609-735, Korea. Tel.: +82 55 350 5298; fax: +82 55 350 5299. *E-mail address:* jaebeom@pusan.ac.kr (JL)

Abstract

In the present study, a rapid, sensitive and quantitative detection of influenza A virus targeting hemagglutinin (HA) was developed using hybrid structure of quantum dots (QDs) and nanoporous gold leaf (NPGL). NPGL film was prepared by dealloying bimetallic film where its surface morphology and roughness were fairly controlled. Anti-influenza A virus HA antibody (ab66189) was bound with NPGL and amine ($-NH_2$) terminated QDs. These biofunctionalized NPGL and QDs formed a complex with the influenza virus A/Beijing/262/95 (H1N1) and the photoluminescence (PL) intensities of QDs were linearly correlated with the concentrations of the virus up to 1 ng/mL while no PL was observed in the absence of the virus, or in bovine serum albumin (BSA, 1 μg/mL) alone. In addition, it was demonstrated that this assay detected successfully influenza virus A/Yokohama/110/2009 (H3N2) that is isolated from a clinical sample, at a concentration of ca. 50 plaque forming units (PFU)/mL. This detection limit is 2-order more sensitive than a commercially available rapid influenza diagnostic test. From these results, the proposed assay may offer a new strategy to monitor influenza virus for public health.

Keywords: nanoporous gold leaf; surface roughness; fluorescence enhancement; quantum dot; influenza A virus

1. Introduction

Epidemic diseases via transmission of the virus are becoming a threatening fear for public health system; e.g., the pandemic influenza A (H1N1) 2009 virus was firstly identified in Mexico in 2009 and caused rapid outbreaks, resulting in ca. 18,000 casualties around the world (Kawai et al., 2012; Panning et al., 2009). It continues to expand globally and causes significant rates of morbidity and mortality, particularly in the elderly and children. A rapid diagnosis of influenza viruses is vital for prevention and timely control of influenza epidemics. Currently forefront tests, i.e., immunosensors and genosensors for monitoring influenza viruses at initial stage usually require professional skill, equipment, multiple processes, and low sensitivity, resulting in retardation to clinical decision (Bonanni et al., 2010; Choi et al., 2010; Deng et al., 2011; Drexler et al., 2009; Druce et al., 2005; Egashira et al., 2008; Kok et al., 2010; Kukol et al., 2008; Owen et al., 2007; Pavlovic et al., 2008; Rahman et al., 2008; van Elden et al., 2001). Numerous technologies for higher sensitivity are emerging for virus detection.

In particular, it has been attractive to utilize photoluminescence (PL) enhancement based on near-field plasmonic effect at metallic nanostructures (Driskell et al., 2011; Gramotnev and Bozhevolnyi, 2010; Schuller et al., 2010). The interaction between metal and semiconductor nanostructure offers attractive opportunities for tuning the optical properties of such composites based on exciton–plasmon coupling. Such composite structures feature complementary optical properties; e.g., semiconductor nanostructures give rise to high emission yields and light-harvesting capabilities, whereas the metallic surface is particularly effective for local probing, confined excitation, non-linear optics and intense PL enhancement (Achermann, 2010; Lee et al., 2006; Lee et al., 2007). Surface roughness has long been considered as one of the critical parameters for optimizing metal enhanced fluorescence and has enabled precise control of localized surface plasmon resonance (LSPR)

74 as well as surface plasmon polariton (SPP). In rough metallic surface, the scattering of SPP

75 mode can produce photons that can decrease diffraction limit and resolve the sub-wavelength

76 structure, thereby unlocking the prospect of utilizing metal-semiconductor nanocomposite

77 films for enhancing PL emission (Ahmed et al., 2012; Leong et al., 2010; Okamoto et al.,

78 2004).

79   Nanoporous gold film has unique physical properties such as excellent stability,

80 biocompatibility, as well as high specific surface area to form self-assembled monolayers

81 from thiols, sulfides and disulfides (Biener et al., 2008; Huang and Sun, 2005). Usually a

82 dealloying technique is utilized to prepare nanoporous structures with controlled pore size

83 and ligaments. By exploiting the dealloying method, PL enhancement in the vicinity of metal

84 nanostructures can be achieved with delicate control of the morphology of the surface on the

85 scale of a few hundreds nanometers in conjunction with interconnected-porous structures

86 (Ciesielski et al., 2008; Detsi et al., 2011).

87   In the present study, the fabrication of metallic surfaces with tunable roughness and

88 controlled structures is reported using the dealloying method. The procedure for fabrication

89 of metal-semiconductor hybrid nanostructures was achieved by means of self-assembly

90 techniques, and the importance of the metallic surface morphology for PL enhancement is

91 illustrated. Furthermore, this physical study expanded to develop a highly sensitive metal-

92 semiconductor hybrid nanostructure for the detection of influenza virus (Fig. 1).

93
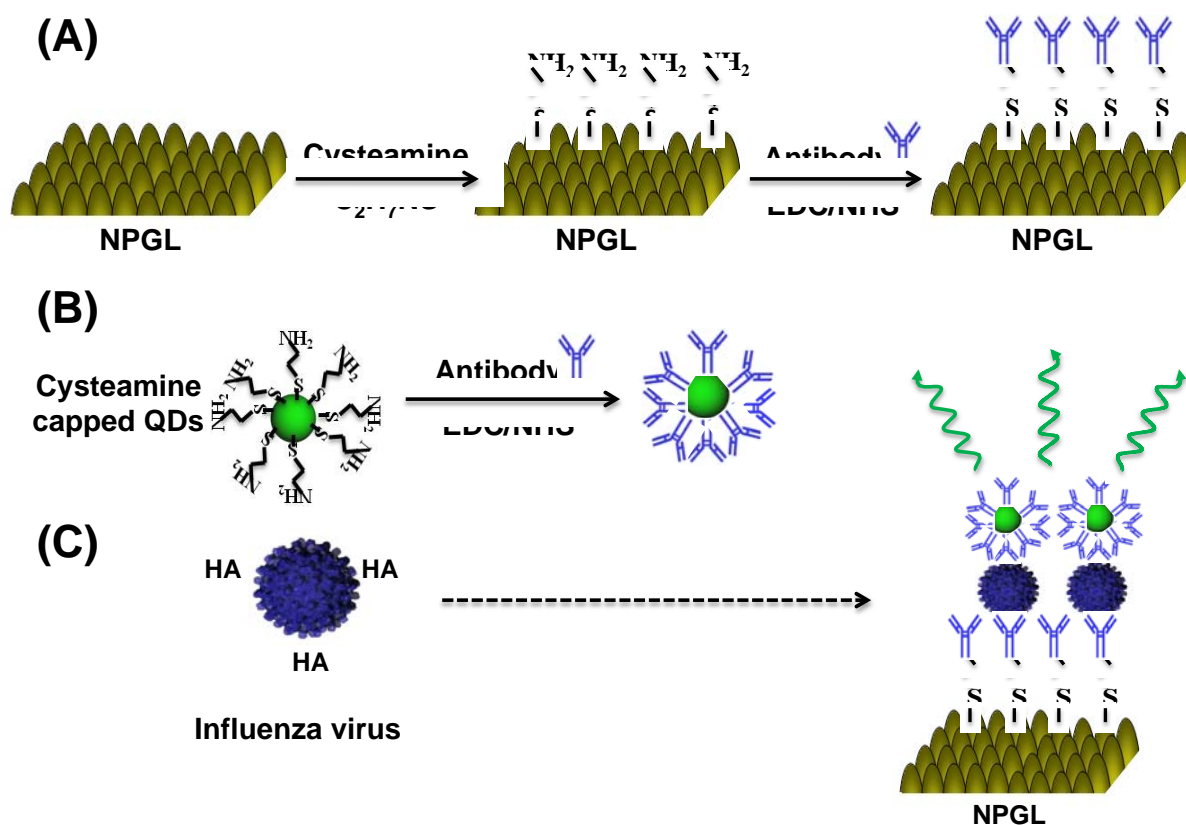
Fig. 1: Schematic of virus detection using nanoporous gold leaf (NPGL) film; The NPGL (A)

and quantum dots (QDs) (B) were firstly conjugated with anti-hemagglutinin (HA) antibodies

(anti-HA Ab, Y shape) by reaction of ethylcarbodiimide (EDC)/*N*-hydroxysuccinimide

(NHS). Then anti-HA Ab-conjugated with NPGL and QDs form complex (C) in presence of

HA on the surface of influenza virus, finally enhancing PL intensity.

2. Materials and methods

2.1. Materials

3-Mercaptopropionic acid (MPA; 99%), poly-diallyldimethylammonium chloride

(PDDA; M.W. 400,000–500,000), poly-acrylic acid (PAA; M.W., ~450,000), cadmium

perchlorate hydrate, thioglycolic acid (TGA), *N*-(3-Dimethylaminopropyl)-*N'*-

ethylcarbodiimide (EDC) and *N*-hydroxysuccinimide (NHS) were purchased from Sigma-Aldrich (Milwaukee, USA). Aluminum telluride (Al_2Te_3) was acquired from Cerac Company (Milwaukee, USA) at the highest purity available. The chromogenic substrate, 3,3′, 5,5′-tetramethylbenzidine (TMB) was obtained from Dojindo (Osaka, Japan). Gold leaf films were purchased from Giusto Manetti Inc. (Campi Bisenzio, Italy). Anti-Influenza A virus HA H1 antibody [B219M] (ab661189, Lot: GR40088-11), anti-Swine Influenza A (H1N1) HA antibody (ab91530, Lot: 942815), and anti-H3 (H3N2) antibody [InA227] (ab82454, Lot: GR84403-3) were purchased from Abcam Inc. (Cambridge, UK). Recombinant influenza A virus HA (H1N1) (New Caledonia/20/1999; Cat: 11683-V08H) and influenza virus A/Beijing/262/95 (H1N1) (Cat: 81N73-2) were purchased from Sino Biological Inc. (Beijing, China) and HyTest Lyd. (Turku, Finland), respectively. Influenza virus A/Yokohama/110/2009 (H3N2) that was isolated from a clinical sample was kindly provided by Dr. C. Kawakami of Yokohama City Institute of Health, Japan and was used for confirming the versatility of the assay system. ECL[TM] anti-mouse IgG, horseradish peroxidase (HRP) linked whole antibody (from sheep) was purchased from GE Healthcare UK Ltd. (Buckinghamshire, UK). All other chemicals were obtained from Wako Pure Chem. Ind. Ltd. (Osaka, Japan). All experiments were carried out using high purity deionized (DI) water (>18 MΩ).

2.2. Preparation of NPGL and semiconductor nanoparticles

The dealloying process of NPGL film has previously been described (Ciesielski et al., 2008). In this study, a gold/silver leaf was gently placed on a microscope slide. This slide was then slowly immersed into a beaker of concentrated nitric acid in order to float the leaf at the air-acid interface. The glass slide was removed when the leaf floated freely on the surface of the nitric acid solution. Subsequently, It was dealloyed for the desired time intervals of 5, 10,

128   30, and 60 min, and labeled as NPGL05, NPGL10, NPGL30 and NPGL60, respectively. The

129   leaf was removed from the acid using a glass slide and transferred it into a beaker containing

130   deionized water, where the leaf was rinsed by floating for 30 min. The dealloyed leaf was

131   withdrawn on a glass substrate that had previously been modified with 3-mercaptopropyl

132   trimethoxysilane in *n*-hexane. TGA-capped cadmium telluride (CdTe) QDs were also

133   synthesized by a technique previously reported in detail (Gaponik et al., 2002) and stored at

134   4°C prior to use.

135   *2.3. Immobilization of CdTe QDs on the NPGL substrate*

136   To evaluate optical properties of NPGL surface, the QDs were immobilized on the NPGL

137   substrate by means of ultrasonic-assisted layer-by-layer (LbL) assembly (Ouyang et al., 2012;

138   Perelshtein et al., 2008) (Supporting information S1). The polymer spacer layer of ca. 20 nm

139   between nanocrystals and metal surface avoids unwanted quenching effects but assists PL

140   enhancement.

141   *2.4. Topographic observation and spectroscopic studies of NPGL films*

142   Topographic images of the NPGL surfaces were obtained using atomic force microscopy

143   (AFM, diInnova, Veeco, USA) and scanning electron microscopy (SEM, S4700, Hitachi

144   High-Technol. Co., Minato-ku, Japan).

145   *2.5. Detection platform of HA, Influenza viruses A/Beijing/262/95 (H1N1), and*

146   *A/Yokohama/110/2009 (H3N2) on NPGL*

147   Antibody specificity for HA (H1N1) was confirmed using an enzyme-linked

148   immunosorbent assay (ELISA) (Supporting information S2) before conjugation to NPGL5

149   film. The anti-HA Ab (ab66189)-conjugated NPGL5 films (Supporting information S3) were

150 rinsed 3 times with phosphate buffered saline (PBS). One hundred μl anti-HA Ab-conjugated

151 QDs (Ab-QDs) (Supporting information S1 and S4) containing different concentrations of

152 recombinant influenza HA (H1N1) was added to the micro plate wells. An Ab-QDs solution

153 in BSA and without influenza virus HA (H1N1) was added to the same micro plate as a

154 negative control. To determine the PL enhancement effect of NPGL05 for HA detection, an

155 identical amount of Ab-QDs solution containing 10 mg/mL HA protein was added to the

156 wells of micro plate. The micro plate was then incubated for 30 min at room temperature. An

157 infinite$^®$ F500 micro plate fluorescence reader (TECAN, Männedorf, Switzerland) was

158 employed to measure the PL intensity of each well. The samples were excited at 380 nm, and

159 the exciting and the emission slits were 5 and 10 nm, respectively. Based on the PL values at

160 different concentration of HA, a dose-dependent curve was constructed. This NPGL-based

161 assay platform was applied on detection of two different types of influenza viruses using the

162 same protocol as described above. Influenza virus A/Beijing/262/95 (H1N1) was detected

163 using anti-HA (H1N1) Ab-bioconjugated NPGL and QDs; influenza virus

164 A/Yokohama/110/2009 (H3N2) was detected using anti-HA (H3N2) Ab-bioconjugated NPGL

165 and QDs.

166 *2.6. Detection of Influenza virus by rapid influenza diagnostic test (RIDT)*

167 To carry out direct and complementary comparison of the detection ability with

168 commercially available influenza diagnostic kit, a commercial RIDT (ImunoAce Flu,

169 TAUNS Lab. Inc., Numazu, Shizuoka, Japan), was purchased to detect Influenza virus

170 A/Yokohama/110/2009 (H3N2) according to manufacturer's protocol. Different virus titers

171 were prepared and then, three drops of virus solution were put on sample port of the testing

172 kit. Positive and negative influenza diagnostic results were obtained from different significant

173 bands that appeared on the strip paper after 10 min of incubation at room temperature.

8

3. Results and discussion

3.1. Topographic observation of NPGL films

SEM images showed that the pore sizes of the substrates varied depending on the dealloying times (Fig. 2a–d). The size of the pores and ligaments increased with longer dealloying times due to increased removal of the less-noble constituent (silver) of the alloy. AFM was used to evaluate the root mean square roughness (R_{rms}) of the surface of each substrate with different dealloying times. The R_{rms} of the substrate was calculated in the scanning area (3 × 3 μm) of the AFM tip. It was found that the shorter dealloying times the small pore sizes, resulting in increasing surface irregularities and the surface roughness. Four selected NPGL samples of variant surface roughness (R_{rms} in lower panel of Fig. 2) were used for further optical evaluation.
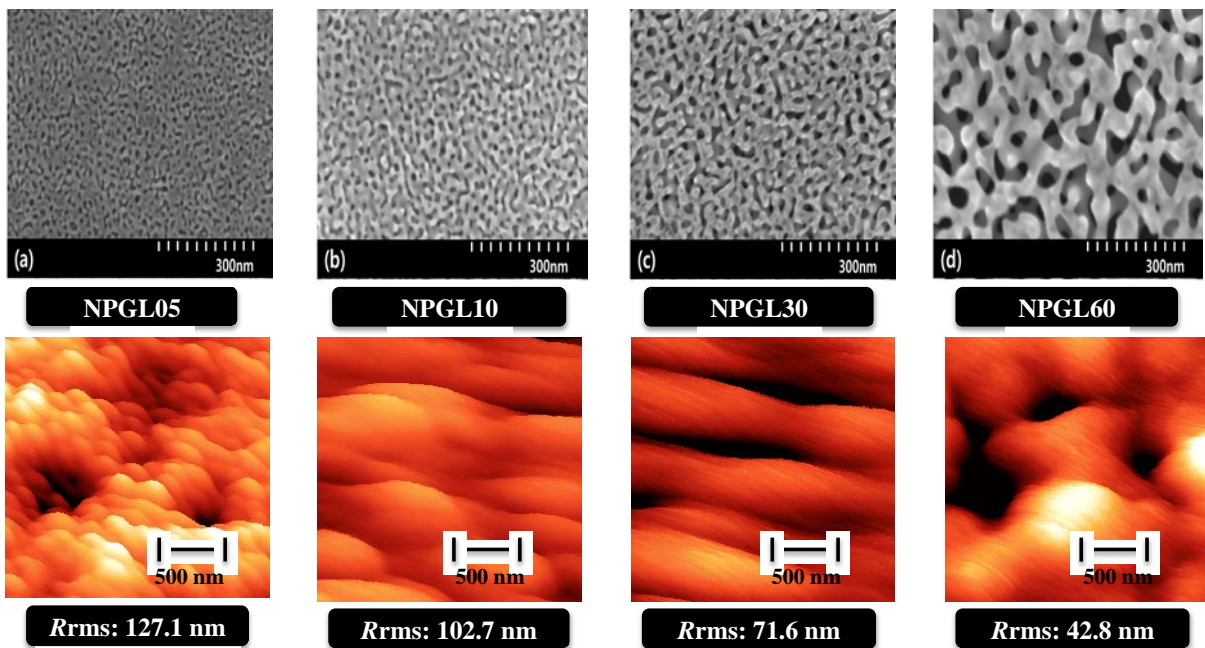
Fig. 2. SEM and AFM images and the measured R_{rms} of each NPGL sample with various dealloying times (5–60 min), where e.g., NPGL05 depicts 5 min of dealloying time. Dealloyed times are 5 min (a), 10 min (b), 30 min (c) and 60 min (d). Bars in upper and lower panels denote 300 and 500 nm respectively.

3.2. Spectroscopic and microscopic studies of the NPGL films

191   The PL band of the synthesized QD solution was observed at 526 nm with a relative

192   quantum yield of > 20% that was determined from the relative ratio vs rhodamine B

193   dispersed in ethylene glycol, where the quantum yield of rhodamine B was 0.95 (Fig. S1A).

194   Given that the surface roughness of each produced NPGL films differed, special care was

195   taken in the QD immobilizing process to ensure that the equivalent amount of QDs was

196   deposited on each substrate. Consequently, it is important to produce a monolayer of QDs on

197   the surface of a metallic substrate. We monitored the absorbance of the QDs on the respective

198   substrates to maintain similar intensities by adjusting the deposition time during the LbL

199   process. Then, the PL intensity of the QD solution at the same absorption of the LbL film was

200   measured. It was observed that the difference in the PL intensity of the various samples was

201   less than 10%, indicating that fairly identical amount of QDs were deposited on the samples

202   (Fig. S1B).

203   Indeed, PL enhancement of QDs on metal surfaces was observed. Fig. 3A shows that the

204   higher roughness the higher PL enhancement; e.g., the emission intensity of QDs on NPGL05

205   (R_{rms} = 127.1 nm) and NPGL60 (R_{rms} = 42.8 nm) was 9- and 2-fold higher than that on a glass

206   substrate, respectively (Fig. 3A). When QDs were deposited on the metal surface without a

207   spacer layer, no PL intensity was observed, rather quenching dominated. This remarkable PL

208   enhancement may be attributed to a strong interaction with surface plasmon of metallic

209   substrate. It has previously been reported that the excitons generated in the QDs can resonate

210   with electron vibrations at the metal surface collectively to induce luminescence

211   enhancement (Lee et al., 2004; Okamoto et al., 2006). Furthermore, the roughness effect on

212   PL enhancement may be related to the multiple scattering phenomena of the SPP mode in

213   combination with rough surfaces. Such roughness and imperfections in nanostructured

214   random media allow SPP of high momentum to scatter and lose momentum and then couple

215 to radioactive light (Okamoto et al., 2006). The fluorescence lifetimes (τ) of the respective

216 samples were measured at an excitation wavelength of 380 nm using a light-emitting diode

217 spectrophotometer (PTI Inc., USA). The spectra in Fig. 3B presents the rougher substrate the

218 shorter lifetime, i.e., the PL lifetime varied from 3.17 ns to 1.2 ns while the R_{rms} values varied

219 from 42.8 to 127.1 nm (Fig. 3C). In contrast, the lifetime of CdTe QDs on glass slides was

220 7.42 ± 0.37 ns. In particular, the short dealloying time generated ultrafine structures that are

221 characterized as small pores and pimples (<10 nm) that play a major role in plasmonic

222 scattering with consequent PL enhancement. Fig. 3D demonstrates a fluorescence

223 microscopic image of the QD/Polymer-deposited films on metallic nano stripe pattern to

224 demonstrate strong PL enhancement induced by metal enhanced fluorescence. With

225 increasing surface roughness, multiple scattering of lights occurs in nanostructured random

226 media. The high enhancement effect observed in close proximity of metallic nanopatterns is

227 primarily due to the absorption and/or emission bands of the QDs overlap with the scattering

228 wavelength of the rough metallic surface. From these fundamental physical experiments

229 NPGR05 substrate was chosen for further sensing experiments of virus detection.

230
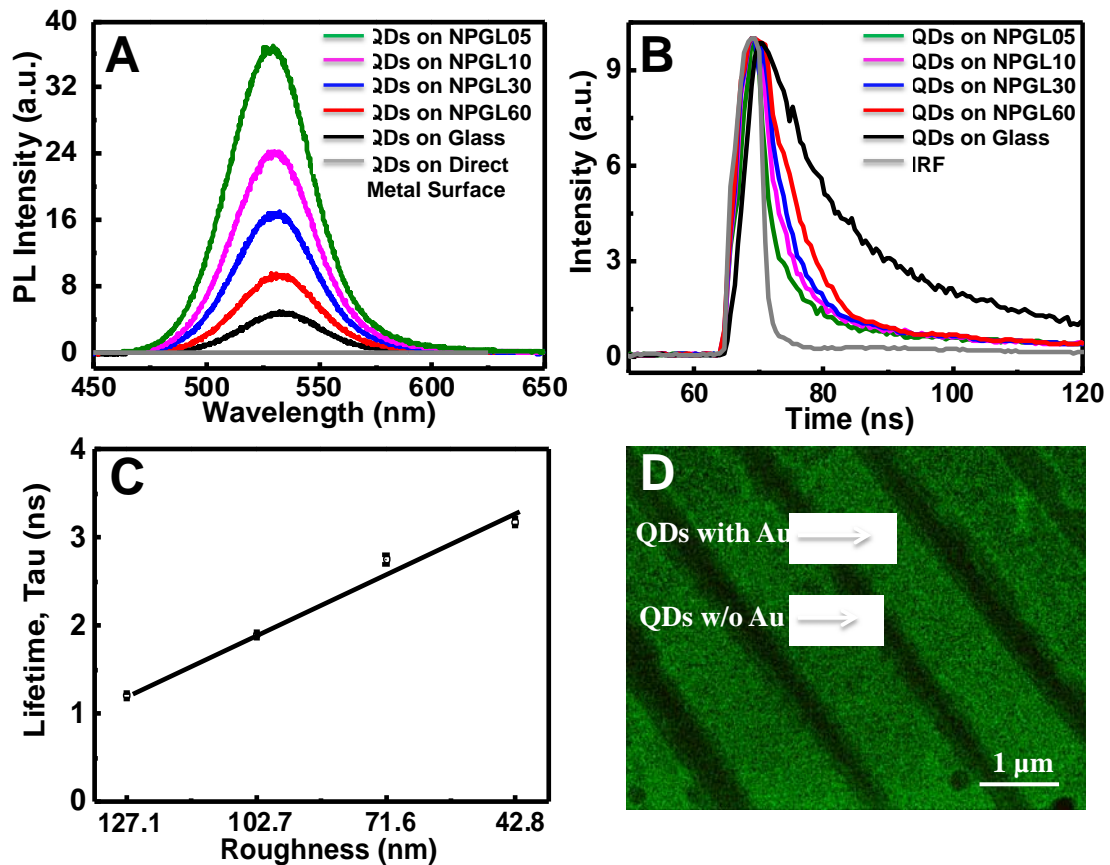
Fig. 3. (A) Photoluminescence (PL) spectra of QDs on different roughness of NPGL and

glass substrate (for QD only); (B) time-based fluorescence kinetics profile of PL signal for

QDs on different surfaces; (C) lifetimes (τ) variance depending on surface roughness; (D)

fluorescence microscopic image of QDs on metallic nano stripe patterns. IRF in (B) stands

for instrumental response function. The error bars in (C) indicate standard deviation (SD) in

each measurement and the scale bar in (D) denotes 1 μm.

3.3. Immunoassay of HA on NPGL05 and QDs

It is known that HA, a surface glycoprotein on the surface of viruses has unique immune-

specificity in the initial stage of infection mechanism (Wiley and Skehel, 1987). The detailed

optical observation at every respective step of bioconjugation with nanomaterials and

241   antibodies was carefully monitored by using ELISA and FTIR spectrophotometry. Immuno-

242   specificity of the anti-HA Ab (ab66189) for influenza virus A/Beijing/262/95 (H1N1) was

243   investigated (Supporting information S1 and S2). A different type of Ab (ab91530) and BSA

244   were used for comparison. A higher absorbance was observed with anti-HA Ab (ab66189)

245   compared to the anti-HA Ab (ab91530) or BSA (Fig. S2A). From these experimental results,

246   anti-HA Ab (ab66189) has a strong immune-specificity for influenza virus A/Beijing/262/95

247   (H1N1) whereas other antibody and BSA show no binding affinity with influenza A virus.

248   ELISA test indicated that the antibodies are successfully conjugated on the NPGLs without

249   losing its binding affinity (Fig. S2B & C). Furthermore, FTIR bands found at 3700-3500 cm^{-1}

250   for amide N-H stretching and 1690-1630 cm^{-1} for amide C=O stretching corresponds the

251   chemical binding between NPGL and anti-HA Ab (ab66189) (Fig. S2D).

252   Then the same experiments were carried out to scrutinize any influence of binding

253   affinity when cysteamine capped QDs were conjugated with anti-HA Ab (ab66189) using

254   recombinant influenza H1N1 HA (New Caledonia/20/1999) (Fig. S3A), resulting that

255   cysteamine capped QDs were successfully conjugated with the antibody (Fig. S3B and C). In

256   fluorescence microscopic image, the aggregated and brighter spot might be virus deposited

257   part on the film (Fig. S3D). The detection procedure consisted of three steps-(i) binding of

258   antibody on NPGL; (ii) binding of antibody on QDs and (iii) immune-reaction between the

259   antibody and antigen.

260   After confirming the binding affinity of antibody on the surface of NPGL film, the

261   recombinant HA (H1N1) was monitored. Both NPGL film and QDs were bound with anti-HA

262   (H1N1) Ab (ab66189), respectively. With HA, these bioconjugated components form a

263   complex, consequently producing high PL intensity from QDs via surface plasmon resonance

264   with the NPGL substrate. In our experiment, 3 times higher PL intensity was monitored in the

265 nanostructure of the antibody-functionalized NPGL than that without the NPGL, where 10

266 μg/mL of HA were added in each experiment (Fig. 4A). In the quantitative analysis using

267 different concentration of HA, PL intensities were logarithmically correspondent on HA

268 concentration in the range of 1 ng/mL to 10 μg/mL (Fig. 4B and the insert). However, there

269 was no significant PL change without any addition of HA or in the addition of BSA.
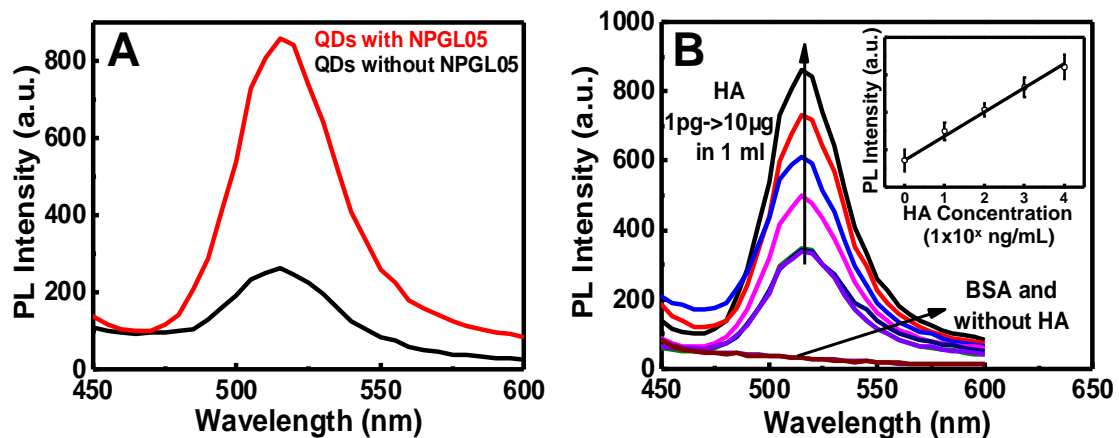
270

271 **Fig. 4.** (A) PL enhancement of QDs with and without the nanostructure; (B) PL enhancement

272 corresponding on different quantities of recombinant influenza HA (H1N1) on anti-HA Ab-

273 conjugated NPGL05. (Insert) the calibration curve of PL intensity versus HA concentration.

274 The error bars indicate SD in each measurement.

275 *3.4. Immunoassay for virus detection*

276   After confirmation of HA monitoring using this novel sensing system with NPGL and

277 QDs, different concentrations of influenza virus A/Beijing/262/95 (H1N1) where the surface

278 of this virus also has specific binding sites of anti-HA (H1N1) Ab was monitored. The similar

279 results were observed as the previous experiment of HA only as shown in Fig. 4B. A

280 significant PL enhancement was observed in the presence of viruses and NPGL (Fig. 5A).

281 Furthermore, a logarithmical relationship existed between PL intensities and the virus

282 concentration in the range of 1 ng/mL to 10 μg/mL (Fig. 5B).

283 Using this developed monitoring system, an influenza virus A/Yokohama/110/2009

284 (H3N2) was monitored. The specificity of HA (H3N2) Ab 82454 for influenza virus

285 A/Yokohama/110/2009 was confirmed (Fig. 5C), and binding of HA (H3N2) Ab 82454 with

286 NPGL05 and QDs was also confirmed using ELISA (Fig. S4). Then, the sensitivity of

287 influenza virus A/Yokohama/110/2009 (H3N2) detection was observed in the range of 50 to

288 10,000 plaque forming units (PFU)/mL (Fig. 5D). The detection limit was shown at ca. 50

289 PFU/mL.
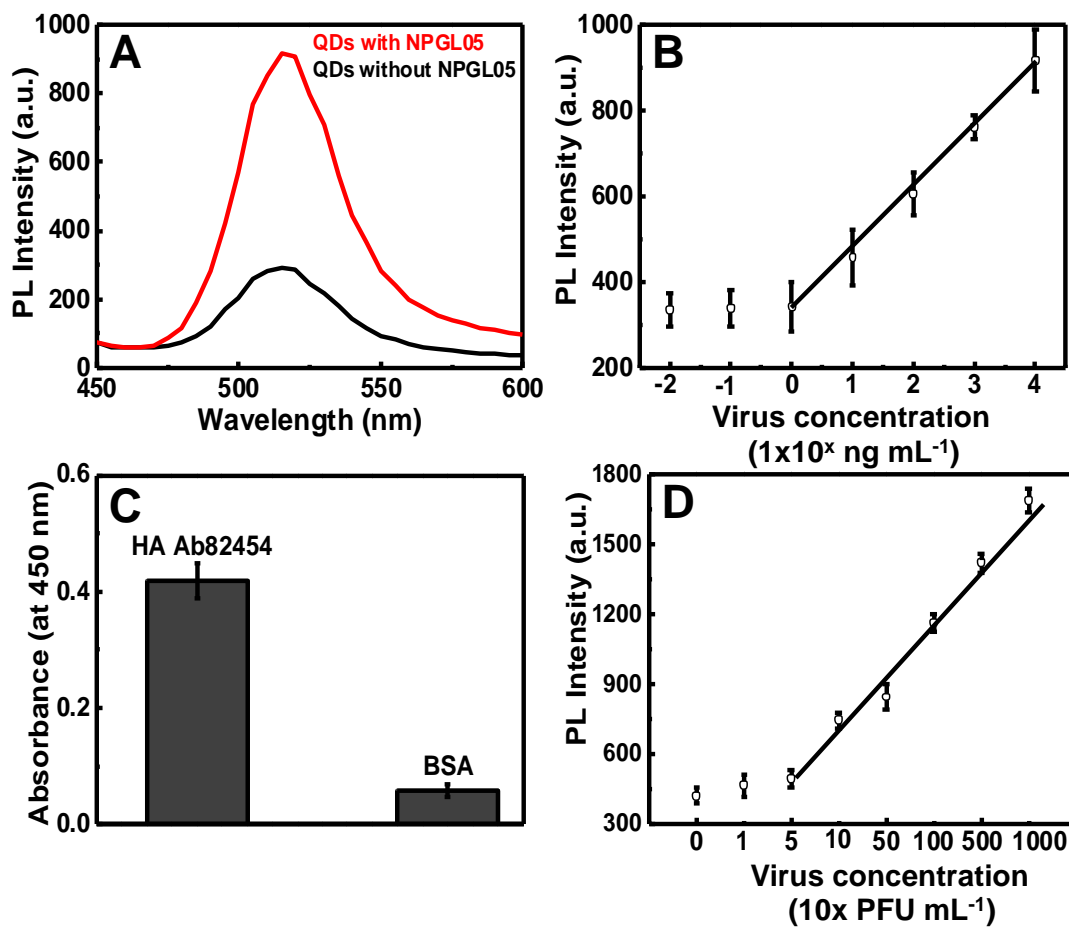
290

291 **Fig. 5.** (A) PL spectroscopic detection of influenza virus A/Beijing/262/95 (H1N1) using

15

292   anti-HA (H1N1) Ab (ab66189)-bioconjugated QDs depending on the existence of anti-HA

293   (H1N1) Ab (ab66189)-bioconjugated NPGL05 film; (B) PL intensity versus influenza virus

294   A/Beijing/262/95 (H1N1) concentration; (C) ELISA results for anti-HA (H3N2) Ab 82454

295   binding with influenza virus A/Yokohama/110/2009 (H3N2); (D) the calibration curve of PL

296   intensity corresponding on the concentration of the influenza virus A/Yokohama/110/2009

297   (H3N2). The error bars in B–D indicate SD (n=3).

298   *3.6. Detection of influenza virus using rapid influenza diagnostic test (RIDT)*

299   A commercially available RIDT kit (ImunoAce Flu, TAUNS Lab. Inc., Numazu,

300   Shizuoka, Japan) was used for comparison with our sensing system to diagnose influenza

301   virus infection using the influenza virus A/Yokohama/110/2009 (H3N2). Table 1 shows the

302   results of the RIDT depending on the concentration of virus. In the case of the commercial

303   RIDT, at least 5000 PFU/mL of virus were required for detection, which means the limit of

304   detection (LOD) of the influenza virus detection using our sensing system of NPGL-QDs was

305   100 times more sensitive than that of the commercial RIDT (Fig. S5).

306   **Table 1: Comparison of influenza virus A/Yokohama/110/2009 (H3N2) detection**

307   **using RIDT**

Detection method	Virus concentration (PFU/mL)								
	10000	5000	1000	500	100	50	10	1	0
This study	+	+	+	+	+	+	–	–	–
Commercial RIDT	+	+	–	–	–	–	–	–	–

308   Note: + and – denote positive and negative diagnoses, respectively.

309   In this study, a new detection method on metallic surface based on exciton-plasmon

310   interaction was presented. In particular, the research of centered on the development of robust

311   rough metallic surfaces that would be used for the generation of high efficient optical device

312 for biosensor applications. Many implications for medical take care require low detection

313 system. An important goal here was to improve detection limit with high sensitivity. As we

314 can see, our proposed detection method showed at least 100 times higher sensitivity than a

315 representative commercial test kit. It might result from the presence of plasmonic rough

316 metallic surface and adjacent control of distance between QDs to induce PL enhancement. In

317 addition, the assay is performed with fewer amounts of reagents and easier to wash out

318 unbound reagents. However, because of the lack of many medical samples, the huge analysis

319 is not attainable using our technique up to now, which will be included in future work.

4. Conclusion

321   This paper reports a near-field optical evaluation of QDs and plasmonic surface

322 composites with varying roughness. A dramatic enhancement of PL intensity and decay rate

323 of the QDs was achieved on rougher metallic surfaces. The observation of these PL

324 enhancements from nanocomposites was further applied for the development of sensitive

325 influenza virus A (H1N1) detection (up to 1 ng/ml) and influenza A (H3N2) virus isolated

326 from a clinical sample (up to 50 PFU/ml). The proposed method represented an alternative

327 traditional method by requiring a higher sensitivity, much smaller sample volume, less

328 amount reagents. Further research will be focused on the development of rough plasmonic

329 metallic surface using self-assembly techniques as well as clinical evaluation.

Appendix A. Supporting information

Supplementary data associated with this article can be found in the online version at

http:// .

References

Achermann, M. 2010. J. Phys. Chem. Lett. 1, 2837–2843.

Ahmed, S.R., Cha, H.R., Park, J.Y., Park, E.Y., Lee, D., Lee, J. 2012. Nanoscale Res. Lett. 7:
438.

Biener, J., Nyce, G.W., Hodge, A.M., Biener, M.M., Hamza, A.V., Maier, S.A. 2008. Adv.
Mater. 20, 1211–1217.

Bonanni, A., Pividori, M.I., del Valle, M. 2010. Analyst 135, 1765–1772.

Choi, Y.J., Kim, H.J., Park, J.S., Oh, M.H., Nam, H.S., Kim, Y.B., Cho, B.K., Ji, M.J., Oh, J.S.
2010. J. Clin. microbiol. 48, 2260–2262.

Ciesielski, P.N., Scott, A.M., Faulkner, C.J., Berron, B.J., Cliffel, D.E., Jennings, G.K. 2008.
ACS Nano 2, 2465–2472.

Deng, Y.M., Caldwell, N., Barr, I.G. 2011. PLoS ONE 6: e23400.

Detsi, E., Schootbrugge, M., Punzhin, S., Onck, P.R., Hosson, J.T.M.D. 2011. Scripta. Mater.
64, 319–322.

359   Drexler, J.F., Helmer, A., Kirberg, H., Reber, U., Panning, M., Müller, M., Höfling, K., Matz,

360   B., Drosten, C., Eis-Hübinger, A.M. 2009. Emerg. Infect. Dis. 15, 1662–1664.

361   Driskell, J.D., Jones, C.A., Tompkins, S.M., Tripp, R.A. 2011. Analyst 136, 3083–3090.

362   Druce, J., Tran, T., Kelly, H., Kaye, M., Chibo, D., Kostecki, R., Amiri, A., Catton, M., Birch,

363   C. 2005. J. Med. Virol. 75, 122–129.

364   Egashira, N., Morita, S., Hifumi, E., Mitoma, Y., Uda, T. 2008. Anal. Chem. 80, 4020–4025.

365   Gaponik, N., Talapin, D.V., Rogach, A.L., Hoppe, K., Shevchenko, E.V., Kornowski, A.,

366   Eychmüller, A., Weller, H. 2002. J. Phys. Chem. B 106, 7177–7185.

367   Gramotnev, D.K., Bozhevolnyi, S.I. 2010. Nat. Photonics 4, 83–91.

368   Huang, J.F., Sun, I.W. 2005. Adv. Funct. Mater. 15, 989–994.

369   Kawai, Y., Kimura, Y., Lezhava, A., Kanamori, H., Usui, K., Hanami, T., Soma, T.,

370   Morlighem, J.E., Saga, S., Ishizu, Y., Aoki, S., Endo, R., Oguchi-Katayama, A., Kogo, Y.,

371   Mitani, Y., Ishidao, T., Kawakami, C., Kurata, H., Furuya, Y., Satito, Y., Okazaki, N.,

372   Chikahira, M., Hayashi, E., Tsuruoka, S., Toguchi, T., Saito, Y., Ban, T., Izumi, S., Uryu,

373   H., Kudo, K., Sakai-Tagawa, Y., Kawaoka, Y., Hirai, A., Hayashizaki, Y., Ishikawa, T.

374   2012. PLoS ONE 7: e30236.

375   Kok, J., Blyth, C.C., Foo, H., Patterson, J., Taylor, J., McPhie, K., Ratnamohan, V.M., Iredell,

376   J.R., Dwyer, D.E. 2010. J. Clin. Microbiol. 48, 290–291.

377   Kukol, A., Li, P., Estrela, P., Ko-Ferrigno, P., Migliorato, P. 2008. Anal. Biochem. 374, 143–

378   153.

379   Lee, J., Govorov, A.X., Dulka, J., Kotov, N.A. 2004. Nano Lett. 4, 2323–2330.

380   Lee, J., Hernandez, P., Lee, J., Govorov, A.O., Kotov, N.A. 2007. Nat. Mater. 6, 291–295.

381   Lee, J., Javed, T., Skeini, T., Govorov, A.O., Bryant, G.W., Kotov, N.A. 2006. Angew. Chem.

382   Int. Edit. 45, 4819–4823.

383   Leong, K., Chen, Y., Masiello, D.J,, Zin, M.T., Hnilova, M., Ma, H., Tamerler, C., Sarikaya,

384   M., Ginger, D.S., Jen, A.K.Y. 2010. Adv. Funct. Mater. 20, 2675–2682.

385 Okamoto, K., Vyawahare, S., Scherer, A. 2006. J. Opt. Soc. Am. B. 23, 1674–1678.

386 Okamoto, K., Niki, I., Shvartser, A., Narukawa, Y., Mukai, T., Scherer, A. 2004. Nat. Mater. 3,

387   601–605.

388 Ouyang, J., Chang, M., Zhang, Y., Li, X. 2012. Thin Solid Films 520, 2994–2999.

389 Owen, T.W., Al-Kaysi, R.O., Bardeen, C.J., Cheng, Q. 2007. Sensor Actuat. B-Chem. 126,

390   691–699.

391 Panning, M., Eickmann, M., Landt, O., Monazahian, M., Ölschläger, S., Baumgarte, S.,

392   Reischl, U., Wenzel, J. J., Niller, H. H., Günther, S. 2009. Eurosurveillance 14, 2003–

393   2008.

394 Pavlovic, E., Lai, R.Y., Wu, T.T., Ferguson, B.S., Sun, R., Plaxco, K.W., Soh, H.T. 2008.

395   Langmuir 24, 1102–1107.

396 Perelshtein, I., Applerot, G., Perkas, N., Guibert, G., Mikhailov, S., Gedanken, A. 2008.

397   Nanotechnol. 19, 245705–245710.

398 Rahman, M., Vandermause, M.F., Kieke, B.A., Belongia, E.A. 2008. Diagn. Microbiol. Infect

399   Dis. 62, 162–166.

400 Schuller, J.A., Barnard, E.S., Cai, W., Jun, Y.C., White, J.S., Brongersma, M.L. 2010. Nat.

401   Mater. 9, 193–204.

402 van Elden, L.J., van Essen, G.A., Boucher, C.A., van Loon, A.M., Nijhuis, M., Schipper, P.,

403   Verheij, T.J., Hoepelman, I.M. 2001. Br. J. Gen. Pract. 51, 630–634.

404 Wiley, D.C., Skehel, J.J. 1987. Ann. Rev. Biochem. 56, 365–394.